Qualitative Differences in the Adsorption Chemistry of Acidic (CO_2, SO_x) and Amphiphilic (NO_x) Species on the Alkaline Earth Oxides

W. F. Schneider*

Physical and Environmental Sciences Department, Ford Motor Company, Mail Drop 3083/SRL, Dearborn, Michigan 48121-2053

Received: August 6, 2003; In Final Form: October 7, 2003

Density functional theory calculations and plane-wave, supercell models are used to examine trends in the adsorption chemistry of CO_2, SO_x ($x = 1, 2$), and NO_x ($x = 1, 2, 3$) on the (001) surfaces of the alkaline earth oxides MgO through BaO. The Lewis acids CO_2 and SO_x adsorb at basic surface oxygen (O_s^{2-}) sites to form local carbonate (CO_3^{2-})-, sulfite (SO_3^{2-})-, and sulfate (SO_4^{2-})-like structures, with adsorption energies increasing uniformly down the series. In contrast, the most stable NO_x-derived anions (nitrite, NO_2^-, and nitrate, NO_3^-) are not formed by Lewis acid−base reactions with acidic (M_s^{2+}) or basic metal oxide surface sites alone. Rather, NO_x adsorption involves both electron transfer and acid−base interactions with the oxide surface that combine to produce acid-like and base-like adsorption states; the increasing oxidizability and reducibility of the alkaline earth oxides contribute to the increasing NO_x adsorption strength down the family. Combining NO_x adsorbates in acidic donor and basic acceptor configurations produces structural modifications and systematically enhanced adsorption energies that arise from interadsorbate charge transfer. These "cooperative" pairs provide qualitatively correct representations of chemisorbed nitrite and nitrate, and comparisons with available experiment support their utility for quantitative description of adsorption energetics as well. The electron transfer and cooperative interactions that distinguish NO_x from SO_x and CO_2 can potentially be exploited to tailor materials selective for NO_x adsorption—an important goal for NO_x emissions control.

Introduction

The interaction of gas molecules with metal oxide surfaces has important environmental[1] and technological significance, in addition to being intrinsically scientifically interesting.[2] The basic metal oxides are commonly used for "scrubbing" acidic gases from combustion emissions, and a particularly significant recent application of this phenomenon is the use of alkaline earth oxides for the selective removal of nitrogen oxides from automotive exhaust containing excess O_2.[3] From a technological point of view, one would like to be able to tailor the properties of these metal oxide adsorbents to, for instance, release a particular adsorbate over a desired temperature range, or to exhibit a particular selectivity for one adsorbate over another. From a scientific perspective, an important first step in this rational design of metal oxide adsorbents is an understanding of the systematics of their interactions with gaseous adsorbates.

The surface chemistry of the cubic alkaline earth oxides (MgO, CaO, SrO, and BaO) is dominated by the Lewis basicity of surface oxide anions (O_s^{2-}).[2] This basicity increases down the alkaline earth family as the metal ions become larger and more electropositive, the crystal lattice expands, and the surface-O-centered valence states rise in energy and become increasingly available for reaction.[4] Lewis acids such as CO_2, SO_2, or SO_3 can be expected to bond to the oxide surfaces at the anion sites, potentially forming surface carbonate (CO_3^{2-}), sulfite (SO_3^{2-}), or sulfate (SO_4^{2-}):[2]

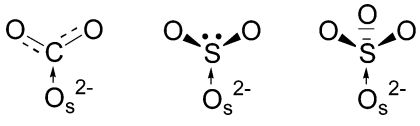

Calculations have verified this general behavior for MgO[5−7] and the other alkaline earth oxides.[4,8] The nitrogen oxides (NO, NO_2, and NO_3) are neither strong Lewis acids nor bases, and their adsorption behavior on the alkaline earth oxides is less straightforward to anticipate than that for CO_2 and SO_x. The most stable NO_x anions are nitrite (NO_2^-) and nitrate (NO_3^-), and if these species are to be formed and stabilized on an oxide surface, it must be through some combination of electron transfer (redox) and acid−base interactions. As a result, adsorption can potentially occur in a variety of modes and, if charge transfer occurs between adsorbates, can exhibit strong adsorbate−adsorbate interaction effects. Charge-transfer-based lateral interactions underlie the "cooperative" effects recently described for NO_x adsorption on MgO;[9] here electron-transfer yields Lewis acidic (NO_x^+) and basic (NO_x^-) adsorbates with both greater surface affinity than the parent neutrals and electrostatic attraction for one another:[10]

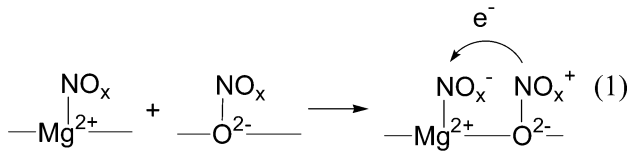

(1)

At least in the case of the (001) surface of MgO, the enhanced surface binding of these "cooperative pairs" can overcome the energetic cost of charge transfer, leading to enhancements in surface bonding on the order of 100%.[9]

In this work, density functional theory (DFT) calculations are used to contrast structures and trends in the adsorption chemistry of the acidic adsorbates CO_2, SO_2, and SO_3 with that of amphiphilic NO, NO_2, and NO_3 on the (001) surfaces of MgO through BaO. The bonding modes are found to be qualitatively constant down the alkaline earth family, with adsorption energies

* E-mail: wschnei2@ford.com.

10.1021/jp036323+ CCC: $27.50
Published on Web 12/09/2003

TABLE 1: PAW/PW91Calculated Bulk and Surface Properties

	lattice constant		bulk modulus	(001) surface relaxation	(001) surface energy
	calc (Å)	expt[a] (Å)	calc (GPa)	calc (M/O, %)	calc (J m^{-2})
MgO	4.248	4.211	149	−0.6/0.6	0.90
CaO	4.832	4.811	107	−1.7/−1.9	0.65
SrO	5.197	5.130	88	−1.8/−2.7	0.51
BaO	5.608	5.523	69	−1.3/−3.1	0.35

[a] Ref. 17.

increasing in parallel with the increasing basicity of the oxides.[8] While simple donor−acceptor concepts adequately describe bonding of the acidic adsorbates, NO_x interacts with the oxide surfaces in both acid-like and base-like modes that are coupled to increasingly pronounced charge transfer down the oxide series. Further, NO_x adsorption is enhanced on all the oxide surfaces through cooperative interactions similar to those found for MgO. For NO_x adsorption on BaO in particular, the results compare favorably with adsorption energies and cooperative interactions inferred from experiment[11] and correlate well with energetics of bulk carbonate, nitrate, and sulfate formation, lending credence to these molecular models and their use for the selection and optimization of oxide adsorbents.

Computational Details

Periodic supercell, plane wave DFT calculations were performed using the VASP code.[12] The interaction of valence electrons with the atomic core states were treated with the projector augmented wave (PAW) method,[13,14] and plane wave basis functions were included to a kinetic energy cutoff of 400 eV. Electronic energies and forces were calculated within the spin-polarized generalized gradient approximation (GGA) using the PW91 functional.[15,16] Appreciable band gaps exist between occupied and virtual states in all the structures considered, and a small (0.005 eV) Gaussian electron smearing was applied only as an aid to electronic convergence.

The alkaline earth oxides (MO) all have the rock salt (NaCl) structure.[17] Table 1 contains the calculated bulk lattice constants and moduli as obtained by fitting to the Murnaghan equation of state. The lattice constants exceed the experimental values by approximately 1%, as is typical for the GGA. The MgO bulk modulus is in line with available experimental and computational results.[18] The (001) surfaces are represented with a slab model similar to that described previously.[9] The tetragonal supercells contain 24 MO formula units arranged in three layers of sixteen ions each (we refer to this as the 2 × 2 surface model, Figure 1). The in-plane repeat distances are derived from the calculated bulk lattice constants, and the repeat distances in the *c* direction are twice the lateral dimension. A 2 × 2 × 1 Monkhorst-Pack mesh is used to sample the first Brillouin zone, which was found to adequately converge the adsorption structures and energies for all four oxides. In all the slab calculations the bottommost layer of ions is fixed at the bulk locations and the remaining ionic positions relaxed using gradient-based optimization until the residual forces were <0.05 eV/Å. All the surfaces closely approximate the bulk terminations, with very slight corrugations and inward relaxations increasing down the family to a maximum of 2−3%. The surface energies (Table 1) are similarly small and decrease down the family.

Adsorption of CO_2, SO_2, SO_3, NO, NO_2, and NO_3 in various configurations were considered on all four oxide surfaces.

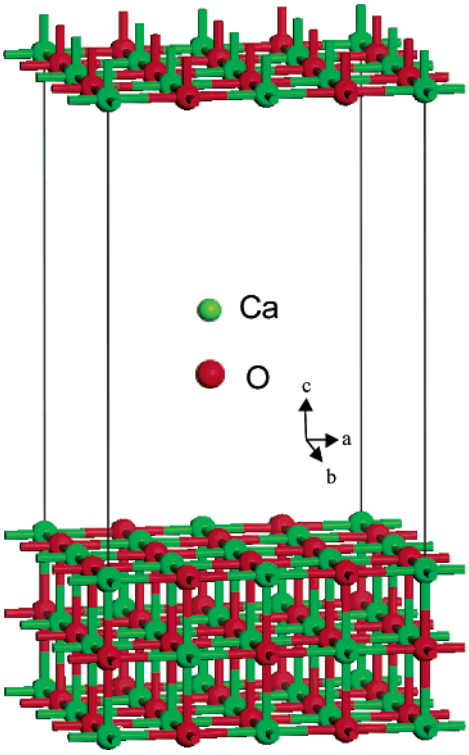

Figure 1. Relaxed CaO supercell, illustrating the 3-layer, 48 atom (4 × 4 × 3) structure employed in all calculations.

Adsorption energies for isolated and cooperative adsorption are calculated using the following expressions:

$$\text{one adsorbate:}\quad \Delta E_{ads} = E^{tot}_{ads+slab} - (E^{tot}_{slab} + E^{tot}_{ads}) \qquad (2)$$

$$\text{two adsorbates:}\quad \Delta E_{ads} = E^{tot}_{ads1+ads2+slab} - (E^{tot}_{slab} + E^{tot}_{ads1} + E^{tot}_{ads2}) \qquad (3)$$

By this convention, $\Delta E_{ads} < 0$ for exothermic adsorption.

Results

CO_2, SO_2, and SO_3 Adsorption. CO_2 is a relatively weak Lewis acid and thus discriminates most strongly between the Lewis base alkaline earth oxides. It is found in all cases to preferentially adsorb on surface O (O_s) to form approximate carbonate-like planar $O_s-CO_2^{2-}$ structures, as shown in Figure 2a for the case of CaO. The tendency toward formation of surface carbonate increases in line with the increase in Lewis basicity down the alkaline earth family. On the weak base MgO-(001), CO_2 physisorbs with an energy of −3 kcal mol^{-1}, consistent with previous cluster model calculations.[4,8,19] This weak adsorption is reflected in the long O_s-C separation and relatively small increase in C−O bond lengths over the calculated gas-phase value of 1.176 Å (Table 2). On the progressively more basic CaO through BaO surfaces, CO_2 chemisorbs with increasing strength (Figure 3). Commensurately the adsorbate geometry becomes increasingly carbonate-like, the C−O bonds lengthening and the O_s-C distance decreasing toward the central value of 1.29 Å typical of bulk carbonates[20] and the O_s-C-O angle approaching the ideal angle of 120°.

SO_2 and SO_3 are more strongly acidic than CO_2 toward the alkaline earth oxides and chemisorb on all the (001) surfaces. SO_2 is a bent molecule with calculated O−S bond lengths of 1.454 Å and an O−S−O angle of 119.5°, and SO_3 is trigonal

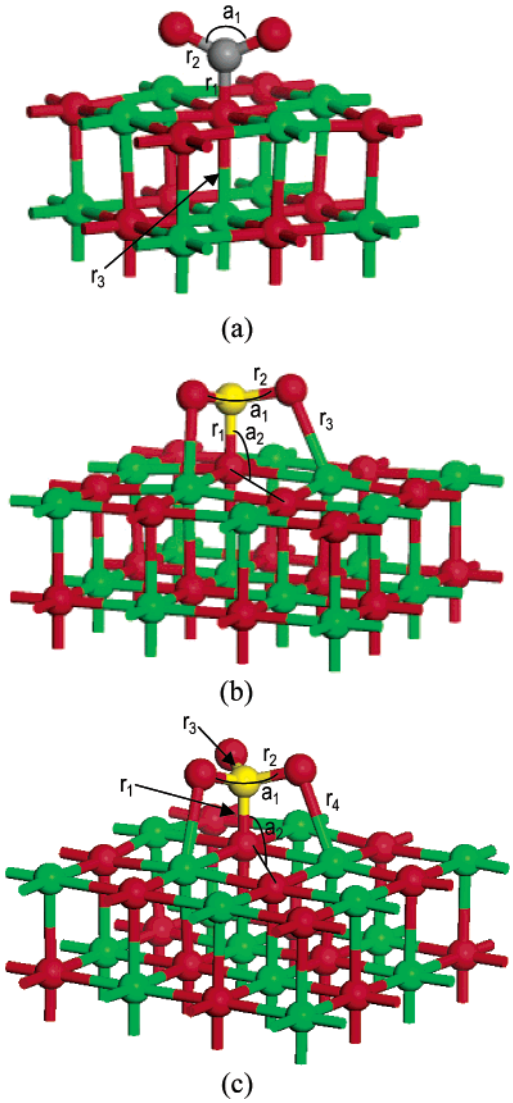

Figure 2. Adsorption geometries of CO_2 (a), SO_2 (b), and SO_3 (c) on CaO(001), representative of other alkaline earth oxides. Geometric parameters given in Table 2.

TABLE 2: Selected Geometric Parameters (distances in Å, angles in deg) of Relaxed CO_2 and SO_x Adsorbates on the (001) Alkaline Earth Oxide Surfaces (See Figure 2 for definitions of parameters.)

		MgO	CaO	SrO	BaO
CO_2	r_1 (O_s−C)	1.475	1.384	1.370	1.358
	r_2 (C−O)	1.250	1.270	1.276	1.282
	a_1 (O−C−O)	134.2	129.1	127.5	126.0
SO_2	r_1 (O_s−S)	1.773	1.708	1.669	1.639
	r_2 (S−O)	1.506	1.510	1.513	1.519
	r_3 (O−M_s)	2.104	2.383	2.565	2.751
	a_1 (O−S−O)	98.6	101.4	102.5	103.6
	a_2 (S−O_s−O_s′)	84.4	93.8	98.1	104.0
SO_3	r_1 (O_s−S)	1.662	1.604	1.587	1.569
	r_2 (S−O)	1.478	1.474	1.478	1.492
	r_3 (S−O’)	1.453	1.482	1.488	1.483
	r_4 (O−M_s)	2.117	2.428	2.582	2.763
	a_1 (O−S−O)	113.0	113.7	113.8	113.3
	a_2 (S−O_s−O_s′)	85.5	94.8	97.3	99.9

planar with a calculated S−O distance of 1.442 Å. As found previously on MgO(001),[5] both preferentially adsorb at basic O_s sites to form approximately pyramidal sulfite-like and approximately tetrahedral sulfate-like surface species, as illustrated in Figure 2b and 2c. The S−O bonds lengthen and

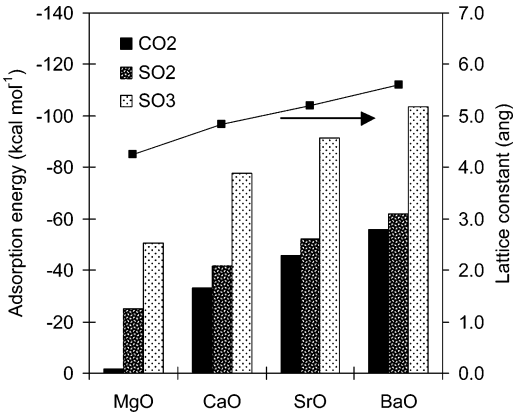

Figure 3. Bulk lattice constants and adsorption energies of Lewis acids on (001) surfaces of the alkaline earth oxides.

TABLE 3: Selected Geometric Parameters (distances in Å, angles in deg) of Relaxed NO_x Adsorbates on the (001) Alkaline Earth Oxide Surfaces (See Figure 4 for definitions of parameters.)

		MgO	CaO	SrO	BaO
NO (acidic)	r_1 (O_s−N)	2.281	1.547	1.502	1.464
	r_2 (N−O)	1.186	1.284	1.298	1.306
	r_3 (O−M_s)	3.511	2.525	2.645	2.806
	a_1 (O_s−N−O)	110.1	108.9	109.8	110.4
NO_2 (acidic)	r_1 (O_s−N)	2.574	1.528	1.465	1.438
	r_2 (N−O)	1.224	1.297	1.310	1.318
	r_3 (O−M_s)	3.28	2.576	2.683	2.834
	a_1 (O−N−O)	129.8	123.1	121.8	120.7
	a_2 (O−N−O_s)	105	110.7	112.2	113.2
NO_2 (basic)	r_1 (M_s−O)	2.268	2.515	2.620	2.748
	r_2 (N−O)	1.237	1.251	1.266	1.276
	a_1 (O−N−O)	124.9	120.9	117.7	115.5
NO_2 (ionic)	r_1 (O_s−N)		3.037	2.796	2.655
	r_2 (N−O)		1.248	1.276	1.276
	r_3 (M−O_s)		2.283	2.356	2.461
	a_1 (O−N−O)		120.8	115.3	116.9
NO_3 (basic)	r_1 (M_s−O)	2.145	2.382	2.542	2.770
	r_2 (N−O)	1.282	1.287	1.287	1.287
	r_3 (N−O’)	1.242	1.240	1.242	1.243
	a_1 (O−N−O)	120.4	119.1	118.7	118.4
	a_2 (O−N−O’)	119.8	120.5	120.7	120.8
NO_3 (ionic)	r_1 (O_s−N)		2.613	2.690	2.798
	r_2 (N−O)		1.272	1.272	1.271
	r_3 (M−O_s)		2.225	2.356	2.504

O−S−O angles narrow uniformly on adsorption, and down the family the adsorbed O_s−S separations (Table 2) approach values typical of bulk sulfite (1.50 Å) and sulfate (1.49 Å),[20] reflecting the increasingly strong surface adsorption (Figure 3). Unlike CO_2, there are pronounced secondary acid−base interactions between the SO_x oxygen and the metal ions (M_s) nearest neighbor to O_s.[8] The S−O bond vectors approximately align toward M_s, and the SO_x fragments tip to achieve an O−M_s separation slightly shorter than the M−O separation in the bulk oxide. These secondary interactions inhibit the free rotation of the adsorbates and lead to an asymmetry in the S−O bond lengths for adsorbed SO_3, resulting in the splitting of the degenerate S−O stretch observed in adsorption of SO_3 on MgO.[5]

In summary, the supercell DFT models find CO_2, SO_2, and SO_3 to adsorb as simple Lewis acids with increasing adsorption strength down the alkaline earth oxide series, consistent with cluster model results.[8]

NO, NO_2, and NO_3 Molecular Adsorption. Because the nitrogen oxides are poor Lewis acids and bases, their adsorption behavior on the alkaline earth oxides is less straightforward to anticipate than that for CO_2 and SO_x. We first consider

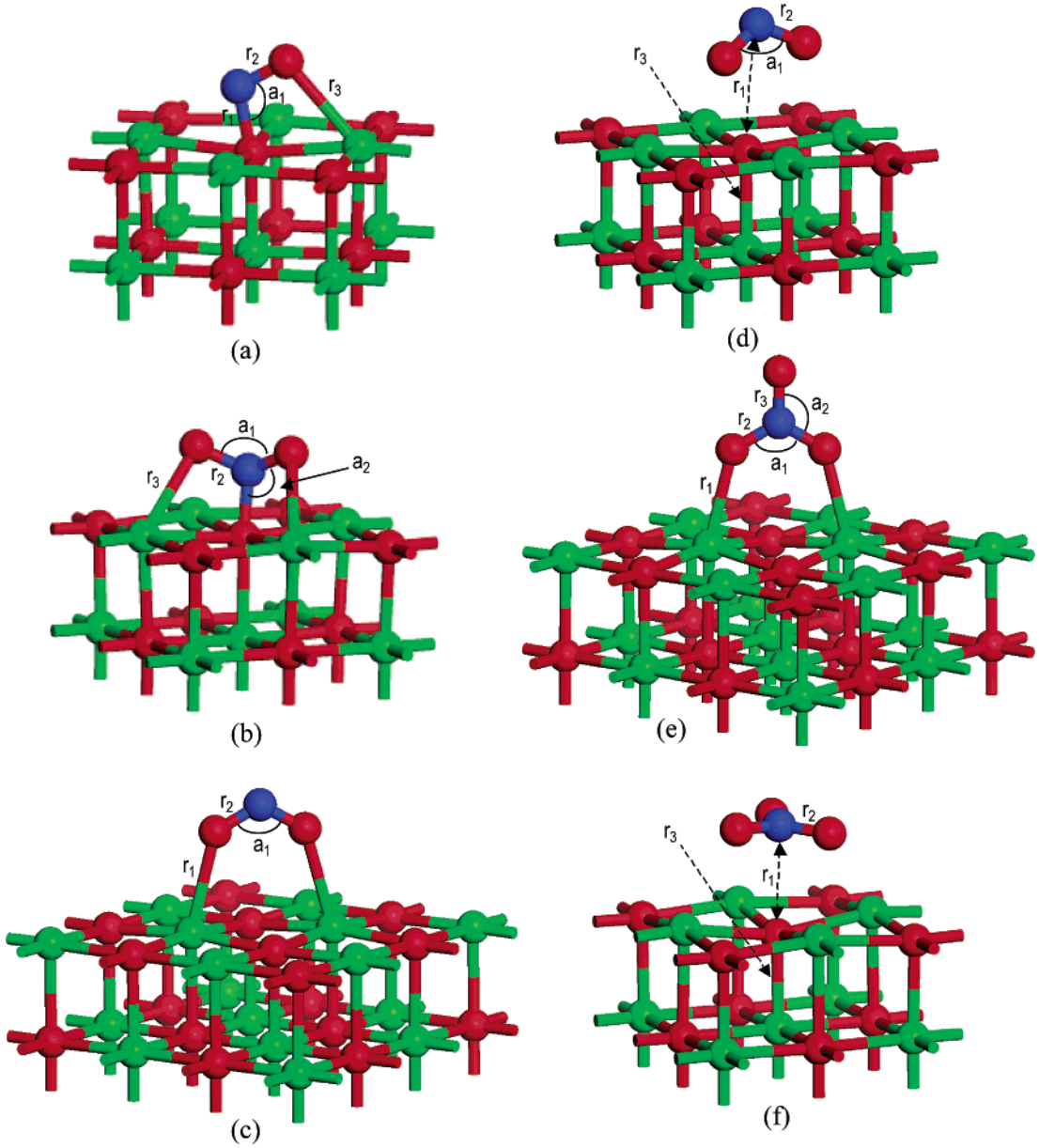

Figure 4. Adsorption geometries of acidic NO (a), acidic NO_2 (b), basic NO_2 (c), ionic NO_2 (d), basic NO_3 (e), and ionic NO_3 (f) on CaO(001), representative of other alkaline earths. Geometric parameters given in Table 3.

adsorption in the limit of low coverage, represented here by a single NO_x adsorbate per supercell, followed by examination of higher coverage and cooperative adsorption effects.

Experiment[21] and theory[9,10,22−24] are in agreement that NO physisorbs on MgO(001) with an energy of about 5 kcal mol^{-1}.[21] Adsorption N-down is preferred over O-down, as is atop O_s over Mg_s, but these preferences are weak and NO sits well above the essentially unperturbed MgO surface.[9,23] Gas-phase NO has a PAW/GGA calculated bond length of 1.169 Å, and adsorption on MgO(001) only slightly increases this separation (Table 3). On the remaining alkaline earth oxides, NO exhibits a more pronounced preference for, and as illustrated in Figure 4a for CaO(001), interacts strongly with basic O_s sites, as has been noted previously in cluster models of CaO.[25] Similar to CO_2 and SO_x adsorption, the O_s−N separation decreases (Table 3) and adsorption energy increases (Figure 5) with increasing oxide basicity. While these trends and the molecular connectivity might suggest an explanation in terms of formation of a surface nitrite (NO_2^-), the O_s−N and N−O bonds are longer by 0.1 Å

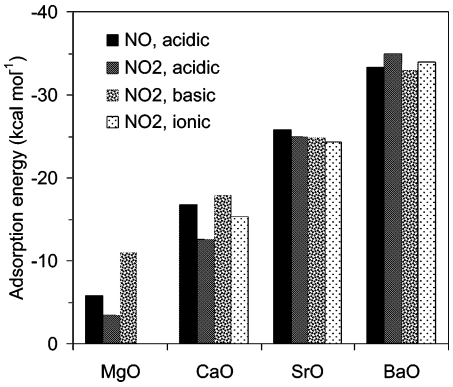

Figure 5. Adsorption energies of isolated NO and NO_2 on (001) surfaces of the alkaline earth oxides.

or more and O_s−N−O angle narrower than those typical of bulk nitrite.[26] NO on O_s^{2-} is formally NO_2^{2-}, i.e., one antibonding and energetically unfavorable electron in excess of the closed-

shell nitrite anion. The ability of the oxides to bind molecular NO as a Lewis acid thus depends both on basicity and on the ability of the surface to accommodate this excess electron:

(acidic NO): $—M^{2+}—O^{2-}—M^{2+}— + NO \longrightarrow$ (4)

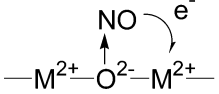

The band gap provides a useful indication of oxide reducibility; from MgO(001) to CaO(001) to SrO(001) to BaO(001) the band gap decreases from 3.7 to 3.2 to 2.7 to 2.3 eV in the models used here. The increase in NO adsorption strength down the alkaline earth oxide family reflects in part the decrease in band gap along the same series.

The NO_2 radical has a very rich coordination chemistry,[26] exhibiting several mono- and bidentate binding modes involving both the N and O centers that reflect its ability to act both as electron donor and acceptor. On the (001) surfaces of MgO[9,10,27,28] and the other alkaline earth oxides,[8,29] two primary adsorption modes have been identified: Lewis-acid-like N-down adsorption on O_s and Lewis-base-like O-down adsorption on M_s, as illustrated in Figure 4b and 4c, respectively. Figure 5 compares the relative stability of these two binding modes down the oxide series.

The acid-like adsorption mode exhibits trends very much like that found for adsorbed NO. On MgO(001), NO_2 physisorbs N-down on O_s, with long O_s−N separation and relatively small perturbations of the N−O bond length and O−N−O bond angle from the calculated gas-phase values of 1.213 Å and 133.7° (Table 3). On the more basic oxide surfaces NO_2 binds more strongly at O_s, with larger relaxations of the NO_2 adsorbate and O_s−N separations more characteristic of a chemisorption bond:

(acidic NO_2): $—M^{2+}—O^{2-}—M^{2+}— + NO_2 \longrightarrow$ (5)

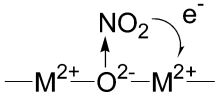

As with NO, the O_s^{2-}−NO_2 fragment has formally one more electron than the closed-shell nitrate anion, NO_3^-, and deviates significantly from the nitrate structure. The ideal nitrate anion is trigonal planar with O−N bond lengths of approximately 1.25 Å;[20] the N−O bond lengths in the O_s^{2-}−NO_2 fragments all exceed the ideal value by 0.05 Å or more and are distinctly nonplanar, with internal O−N−O angles summing to approximately 345°, or 15° less than the ideal value (Table 3). Again, part of the increasing adsorption strength in this acidic mode down the oxide series can be attributed to more ready delocalization of the "excess" electron to the oxide conduction band. Cluster[8] and other supercell models[29] predict longer O_s−NO_2 distances than those found here, likely the result of smaller and more restrictive surface models.

The most favorable base-like adsorption mode bridges two M_s in the [110] direction (Figure 4c).[8−10] This O-down mode is favored by 8 kcal mol^{-1} over the N-down mode on the MgO(001) surface and increases in adsorption strength down the series (Figure 5) but at a rate less than the N-down mode, which becomes slightly preferred in these surface models at SrO. NO_2, with a gas-phase electron affinity of 2.27 eV,[30] is a rather strong oxidizer, and this adsorption mode probes both the Lewis acidity and oxidizability of the oxide surface:

(basic NO_2): $—M^{2+}—O^{2-}—M^{2+}— + NO_2 \longrightarrow$ (6)

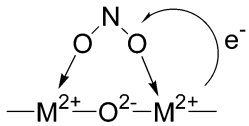

Down the series the N−O bonds lengthen and O−N−O angles increase (Table 3) in a fashion that reflects the increasing charge transfer to the adsorbate.

As the alkaline earth oxides become both more easily oxidized and the metal ion centers become less acidic down the series, a third adsorption mode begins to compete with the two above. This "ionic" mode results from pairing of a one-electron-reduced NO_2 adsorbate with an electron hole localized on an O_s ion:

(ionic NO_2): $—M^{2+}—O^{2-}—M^{2+}— + NO_2 \longrightarrow$ (7)

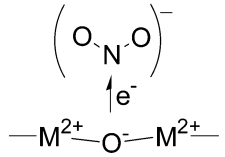

Simple electrostatic analysis demonstrates that a negatively charged ion will be attracted preferentially to an electron hole site on an otherwise undefected square ionic lattice; this electrostatic interaction largely accounts for the NO_2 binding in this mode. As shown in Figure 4d and Table 3, the ionic binding mode is characterized by a large relaxation of the "O^-" center into the surface, relatively large separation and nonspecific interaction of the adsorbate with the surface, and NO_2 geometric parameters consistent with a "nitrite" description. This adsorption mode is sensitive to surface oxidizatility and competes most directly with the basic adsorption mode: on the large band gap and relatively acidic MgO(001) surface only the basic adsorption mode is present; on the increasingly basic oxides the ionic mode gains in stability (Figure 5) until at BaO(001) it is actually slightly preferred to the basic one. As has been previously noted, in a purely ionic description, the O^{2-} ion owes its stability to the Madelung potential of surrounding ions; as the lattice constant increases and this stabilizing potential decreases, conversion to O^- (a highly exothermic process in the gas-phase) becomes increasingly easier.[31]

The NO_3 radical is a highly reactive species and in the gas phase is thermodynamically unstable (by 9 kcal mol^{-1}) with respect to decomposition to NO_2 and O_2. Interactions with an oxide surface can act to stabilize NO_3, and thus it is an important species to consider as a participant in NO_x surface chemistry on oxides. The NO_3 radical has a gas-phase electron affinity of 3.94 eV,[30] making it an even stronger oxidizer than the NO_2 radical, but in its neutral form is a very poor Lewis acid; its surface bonding is thus influenced by factors similar to the basic and ionic NO_2 modes. Thus, NO_3 adsorbs in a basic fashion O-down and bridging two M_s in the [110] diagonal on all four metal oxide surfaces (Figure 4e):[8−10]

(basic NO_3): $—M^{2+}—O^{2-}—M^{2+}— + NO_3 \longrightarrow$ (8)

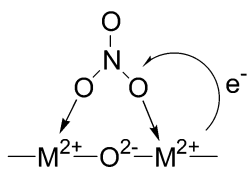

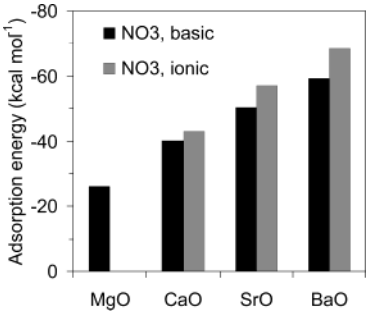

Figure 6. Adsorption energies of isolated NO_3 on (001) surfaces of the alkaline earth oxides.

as well as atop an O_s in an ionic fashion on all the oxides save MgO (Figure 4f):

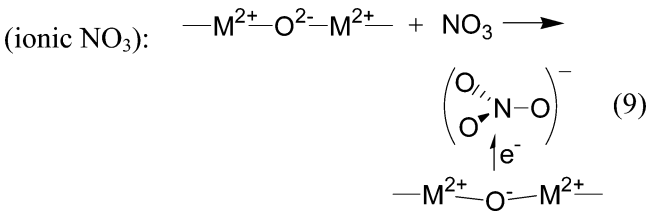

(9)

NO_3 as an adsorbate shows a remarkable consistency in structure down the oxide series: in the basic adsorption modes (Table 3) the NO_3 fragments are planar with internal angles nearly exactly 120° and N−O bond lengths close to 1.25 Å, i.e., nearly ideal for a nitrate anion. Mulliken charge analysis shows that charge transfer from the surface to the adsorbate is nearly complete on MgO(001)[9,10] and the higher members of the series.[8] Similarly in the ionic mode, the NO_3 fragment has nearly ideal D_{3h} symmetry and sits flat and centered directly above an O_s that is relaxed into the surface. Because of this strong charge-transfer effect, an isolated NO_3 is predicted to bind by more than 25 kcal mol^{-1} on all the oxide surfaces (Figure 6), more than sufficient to stabilize NO_3 against decomposition to adsorbed NO_2 and molecular O_2. On the more acidic MgO-(001) surface, adsorption only occurs via the basic mode; on the remaining surfaces both modes are present, with the ionic ones becoming increasingly preferred down the series.

NO_x Cooperative Adsorption. As shown above, the molecular adsorption modes of isolated NO_x species are largely controlled by one-electron exchanges with the oxide surfaces. The alkaline earth oxides are neither particularly good oxidants nor reductants; not surprisingly, isolated NO_x is predicted to chemisorb more readily near oxidizable or reducible defects than to an undefected surface.[10,25,32] However, surface defects alone cannot account for the ready and extensive chemisorption of NO_2 observed even on MgO(001).[22,27] Rather, we have previously considered a cooperative representation of chemisorbed NO_x on MgO(001), in which acid- and base-bound adsorbates couple to form more strongly bound pairs:[9]

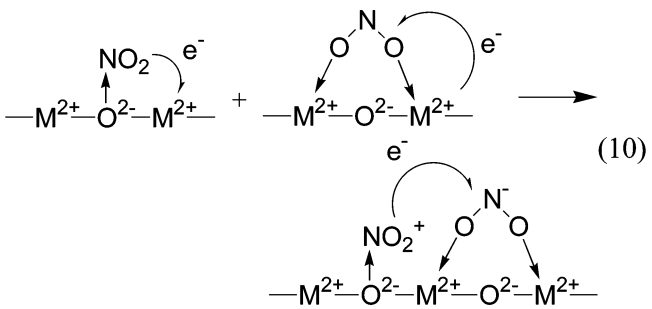

(10)

TABLE 4: Selected Geometric Parameters (distances in Å, angles in deg) of Relaxed NO/NO_2 Pairs on the (001) Alkaline Earth Oxide Surfaces (See Figure 7 for definitions of parameters.)

			MgO	CaO	SrO	BaO
NO/NO_2	NO	r_1 (O_s−N)	1.432	1.378	1.351	1.331
	(acidic)	r_2 (N−O)	1.207	1.223	1.233	1.241
		r_3 (O−M_s)	2.312	2.629	2.874	3.098
		a_1 (O_s−N−O)	111.0	113.2	114.0	114.9
	NO_2	r_4 (M_s−O)	2.106	2.381	2.533	2.708
	(basic)	r_5 (N−O)	1.276	1.276	1.278	1.279
		a_2 (O−N−O)	116.2	115.5	115.3	115.2
NO_2/NO_2	NO_2	r_1 (O_s−N)	1.410	1.364	1.347	1.328
	(acidic)	r_2 (N−O)	1.219, 1.236	1.240	1.245	1.252
		a_1 (O−N−O)	129.3	126.4	125.0	123.6
		a_2 (O−N−O_s)	116.6, 114.1	116.8	117.5	118.2
	NO_2	r_3 (M_s−O)	2.100	2.381	2.529	2.704
	(basic)	r_4 (N−O)	1.275	1.276	1.276	1.278
		a_3 (O−N−O)	116.4	115.5	115.3	115.1
NO_2/NO_3	NO_2	r_1 (O_s−N)	1.412	1.365	1.348	1.329
	(acidic)	r_2 (N−O)	1.218, 1.235	1.240	1.245	1.251
		a_1 (O−N−O)	129.4	126.4	125.0	123.6
		a_2 (O−N−O_s)	116.6, 114.0	116.8	117.5	118.2
	NO_3	r_3 (M_s−O)	2.099	2.380	2.531	2.708
	(basic)	r_4 (N−O)	1.288	1.288	1.288	1.290
		r_5 (N−O')	1.233	1.237	1.239	1.239
		a_3 (O−N−O)	119.5	118.6	118.4	118.1
		a_4 (O−N−O')	120.5	120.7	120.8	121.0
NO_2/NO_3	NO_2	r_1 (O_s−N)		1.359	1.341	1.321
	(acidic)	r_2 (N−O)		1.241	1.246	1.252
		a_1 (O−N−O)		125.7	125.0	123.9
		a_2 (O−N−O_s)		117.1	117.8	117.9
	NO_3	r_3 (O_s−N)		2.557	2.633	2.768
	(ionic)	r_4 (N−O)		1.278	1.279	1.281
		r_5 (O_s−M)		2.207	2.360	2.532

In effect, charge transfer between adsorbates substitutes for charge transfer between adsorbate and surface. On MgO(001), this cooperative adsorption effect enhances adsorption energies of NO (acid)/NO_2 (base), NO_2 (acid)/NO_2 (base), and NO_2 (acid)/NO_3 (base) pairs by approximately a factor of 2. These pairs thus provide plausible models for chemisorbed nitrite and nitrate on MgO. The more basic members of the alkaline earth oxide series adsorb neutral NO_x much more strongly than does MgO, and the contribution of cooperativity to adsorption on these oxides remains to be determined. This question is considered here for NO_x pairs on all four of the (001) oxide surfaces.

The configuration space for pairs of adsorbates is much larger than that for single adsorbates, as the pairs can reside at nearest-neighbor, next nearest-neighbor, etc., sites, and at each site the adsorbates can interact with the surface in a variety of modes. These geometric effects have been examined for cooperative NO_x adsorption on MgO(001),[9] and here we consider structures analogous to those identified previously, including NO/NO_2, NO_2/NO_2, and NO_2/NO_3 pairs formed from combinations of the acidic and basic adsorption modes described above. In addition, we consider an NO_2/NO_3 pair with the NO_3 fragment in the ionic binding geometry. Figure 7a−d shows representative relaxed adsorption geometries for these four configurations, and structural parameters are provided in Table 4.

In all cases considered, the electronic, structural, and energetic evidence all point toward a cooperative enhancement of adsorption on all the alkaline earth oxides. Most readily apparent are the pronounced structural relaxations that accompany pair wise NO_x adsorption. For example, in the case of acidic NO adsorbing on O_s and basic NO_2 on nearby M_s, both adsorbates relax into the surface relative to the isolated species (cf. Tables 3 and 4). On MgO(001), on which isolated NO and NO_2 weakly physisorb, the inward relaxations are dramatic—0.15 Å for NO_2

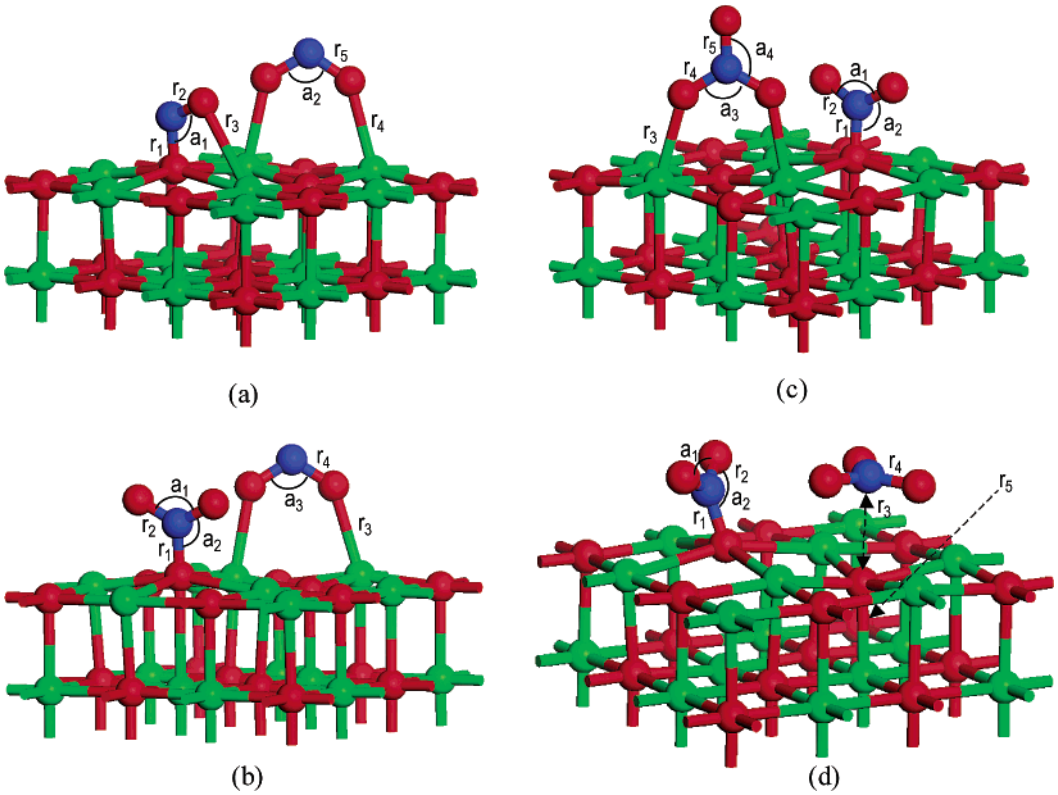

Figure 7. Adsorption geometries of NO (acid)/NO_2 (base) (a), NO_2 (acid)/NO_2 (base) (b), NO_2 (acid)/NO_3 (base) (c), and NO_2 (acid)/NO_3 (ionic) (d) cooperative pairs on CaO(001), representative of other alkaline earths. Geometric parameters given in Table 4.

and more than 0.8 Å for NO—while on the remaining alkaline earth oxides the relaxations are smaller but still quite significant—0.04 and 0.13 Å for NO_2 and NO on BaO(001), respectively. In addition to this overall inward relaxation, the N−O bonds in the O_s−NO fragments shorten and the O_s−N−O angles widen to values more consistent with that of a nitrite (NO_2^-) anion, i.e., of a fragment oxidized by one electron. In parallel, the N−O bonds in the NO_2 fragments expand and the O−N−O angles narrow to values also typical of nitrite anion, i.e., of fragment reduction by one electron. The spontaneous pairing of electron spins that is observed further shows that a charge transfer between adsorbates underlies these structural modifications. The ground state of the system would be expected to be magnetic if there was no electron transfer between adsorbates; rather, the Fermi gap for the adsorbed NO/NO_2 pairs is approximately 0.6 eV (14 kcal mol^{-1}), which provides a rough indication of the energy gain from spin pairing.

Similar structural and electronic effects are found for the NO_2/NO_2 and NO_2/NO_3 pairs (Figure 7b,c,d and Table 4). In the first case, the O_s-bound (acidic) NO_2 relaxes inward as much as noted above for NO. Further, the pyramidalized N center flattens to produce an approximately trigonal planar O_s−NO_2 fragment, consistent with that expected for a nitrate (NO_3^-) anion. On MgO(001) this fragment tilts toward a neighboring M_s, while on the remainder of the oxides it sits nearly directly above the O_s. The partner M_s-bound NO_2 fragments adopt geometries nearly identical to that found in the NO/NO_2 pairs, and the net result is a cooperative pair of nitrate and nitrite. Likewise for the NO_2/NO_3 combinations, the O_s-bound NO_2 relaxes inward and becomes planar and nitrate-like. The NO_3 fragments, in contrast, relax inward somewhat but are otherwise little changed from the structures found for isolated NO_3 on these oxides. As noted above, NO_3 is a strong enough oxidant to extract an electron from the oxide surface itself; a nearby

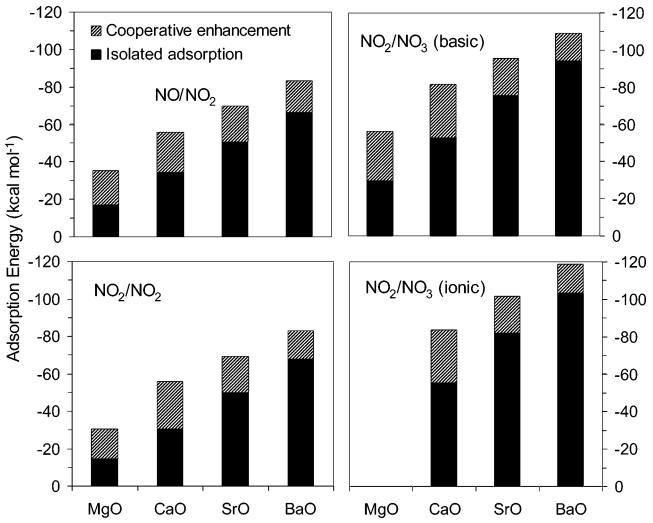

Figure 8. Total adsorption energies of isolated adsorbates (solid bars) and cooperative enhancement (hashed bars).

NO_2 provides a more ready source of an electron, but does not change the structure of the resultant NO_3^--like adduct.

Figure 8 shows the total adsorption energy of the cooperative pairs, decomposed into the isolated adsorption energies (solid bars) and net cooperative enhancement energy corresponding to reaction 1 (hashed bars). As observed above for all the isolated adsorbates, the absolute adsorption energies increase down the alkaline earth family in line with the general increase in oxide basicity. The NO/NO_2 and NO_2/NO_2 pairs have comparable adsorption energies, in line with the behavior found for isolated NO and NO_2 (Figure 5), while the NO_2/NO_3 pairs adsorb approximately 25 kcal mol^{-1} more strongly. The NO_3 fragment shows a slight preference for the ionic configuration over the M_s-bridging basic one, ranging from 2 kcal mol^{-1} for

CaO to 10 kcal mol^{-1} for BaO and consistent with the preferences found for isolated NO_3. The net cooperative enhancement is nearly constant across all oxides and adsorbate pairs, rising only slightly from MgO to CaO and then dropping to SrO and BaO. The enhancement is a balance between the energy cost of electron transfer between adsorbates and the adsorption energy gain from electron transfer; these two apparently balance one another down the series. The net result is a decrease in the relative magnitude of the cooperative effect down the oxide series, from nearly 100% increase in adsorption strength at MgO to approximately 20% enhancement at BaO. We have not examined cooperativity on other types of surfaces structures, e.g., steps, but it seems likely that cooperativity will similarly be a constant addition on top of the (greater) adsorption energy of the isolated adsorbates.

The NO_2/NO_3 (ionic) configuration (Figure 7d) shows a cooperative enhancement comparable to that found for the NO_2/NO_3 (base) pair (Figure 7c). This enhancement is perhaps surprising on the basis of the descriptions of the ionic binding mode (eq 9) and cooperative enhancement (eq 10) given above: charge transfer from NO_2 to NO_3 would seemingly disrupt the $O_s^- - NO_3^-$ interaction that underlies the ionic bonding mode and should thus diminish the surface−adsorbate bonding. The observed bonding enhancement involves couplings between adsorbate−adsorbate and adsorbate-oxide charge transfer that are not captured in the simple one-electron-transfer pictures. The Fermi gap in the NO_2/NO_3 (ionic) pairs is narrower than in the NO_2/NO_3 (base) ones, reflecting greater mixing of surface and adsorbate states. Further charge and orbital analysis will be helpful in unraveling the components of ionic and cooperative bonding on the more basic oxides.

Finally, the large electrostatic contributions to NO_x binding, in particular in the ionic binding modes, suggests a potential sensitivity to supercell dimensions and slab thickness. Test calculations with varied supercell dimensions demonstrate that the reported results are robust to these model choices. While the relative stabilities of the various bonding modes may be sensitive to details of the surface models, the qualitative features are not.

Discussion

The qualitative picture that emerges from these results is of alkaline earth oxide surface chemistry controlled by a combination of Lewis acid/base (electron pair acceptor/donor) and one-electron-transfer interactions. The picture is simple and predictable for the Lewis acids CO_2, SO_2, and SO_3, where adsorption occurs at Lewis basic O_s^{2-} sites to form surface-bound carbonate, sulfite, and sulfate anions, respectively. These are primarily dative interactions, with O_s^{2-} lone pair electrons filling vacant adsorbate acceptor orbitals. The driving force for adsorption increases down the alkaline earth family in line with the increase in basicity with lattice constant,[4,8] or in a different language with improving energy match and overlap between donor and acceptor states.[33] At low to moderate coverages the adsorbates are not expected to interact with one another accept through destabilizing lateral steric repulsions.

The picture becomes more complicated for the nitrogen oxides, where chemisorption to produce nitrite or nitrate must be coupled to one-electron-transfer processes. The relevance of redox chemistry is apparent from the observation that nitrogen atoms in molecular NO, NO_2, and NO_3 are in even oxidation states (2+, 4+, and 6+, respectively) while the nitrogen oxidation states in the nitrite and nitrate anions are odd (3+ and 5+, respectively). Thus, NO and NO_2 do not mimic CO_2 or SO_x by simply adding as Lewis acids to O_s^{2-} to form nitrite or nitrate. Rather, NO and NO_2 on O_s^{2-} are one electron in excess of the corresponding NO_x anions, and adsorption is enhanced by electron delocalization. In the absence of other sinks the oxide surface itself accommodates the extra electron, and its ability to do so is reflected in the increasing adsorption strength of the isolated adsorbates on O_s down the alkaline earth series.

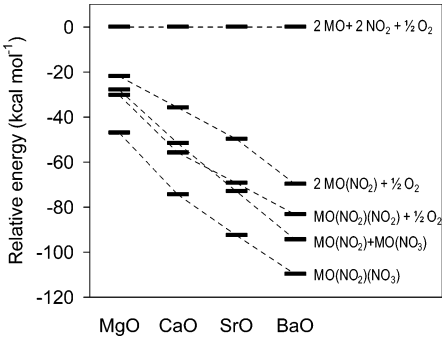

Figure 9. Stabilities of molecular and cooperative NO_x adsorbates on the alkaline earth oxides relative to gas-phase NO_2 and O_2.

An alternative electron sink is a nearby NO_x, and formation of paired and surface-bound $O_s^{2-} - NO_x^+$ and NO_x^- underlies the cooperative chemisorption effect. The cooperative model predicts the existence of a variety of NO_x surface species on exposure of an alkaline earth oxide to NO_x and is consistent with a variable surface stoichiometry arising from mixtures of these species. For instance, Figure 7 illustrates two types of surface nitrite and three of surface nitrate, and Figure 7b shows a mixed nitrite/nitrate surface accessible simply from (cooperative) adsorption of NO_2. Other proportions, and in fact other adsorption geometries for the acidic and especially the basic NO_x components, are possible. The cooperative effect is a stabilizing lateral interaction between NO_x neighbors. We have explored the effect at fairly low NO_x coverage; more complicated electronic interactions are possible as coverage increases and more neighbors interact, but as shown through comparison with experiment below, the models here appear to capture the most important physical processes that govern reactivity.

Figure 9 compares the relative stabilities of the NO_2-derived isolated and cooperative adsorbates down the alkaline earth oxide family. (The lowest energy configurations for each surface stoichiometry are reported, and the experimental $NO_2 + {}^1/_2O_2 \rightarrow NO_3$ energy of 9 kcal mol^{-1} is used to put the various adsorbates on the same energy scale.) Apparent are the driving force for $NO_2 \rightarrow NO_3$ oxidation provided by surface adsorption and the adsorption enhancement provided by cooperative interactions. These combine to produce a rich and complicated NO_x surface chemistry. Numerous experimental studies provide qualitative support for this picture, including the observation of mixtures of NO_x surface species on NO_2-exposed MgO[27,28] and BaO thin films[34] and mixed BaO/MgO powders,[35] In fact, complicated NO_x surface species were noted in very early work on CaO powder as an NO adsorbant.[36] Outside the alkaline earth family, NO_2 has been found to form mixtures of nitrite and nitrate species on Al_2O_3, TiO_2, and Fe_2O_3 powders.[37]

The spectroscopic observations are consistent with the existence of various interacting NO_x adsorption modes as presented here but do not provide a quantitative test of the results. Little quantitative analysis of NO_x uptake by well-defined oxide substrates is available, but the flow reactor and kinetic modeling studies of NO_x uptake by baria supported on alumina reported by Fridell and co-workers do provide one

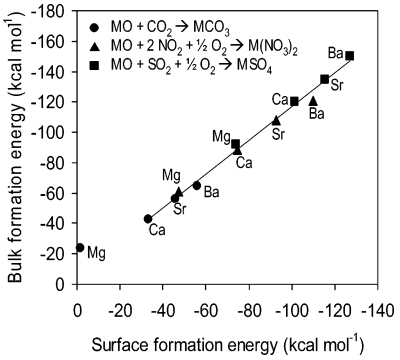

Figure 10. Comparison of calculated surface and experimental bulk formation energies.

TABLE 5: Comparison of Experimentally Inferred ($E_a^f - E_a^r$)[11] and Calculated NO_x Adsorption Reaction Energies (kcal mol^{-1})

	expt	calc
[BaO] + NO_2 → [BaO]−NO_2	−38	−35
[BaO] + $2NO_2$ → [BaO]−NO_3 + NO	−33	−43
[BaO]−NO_3 + NO_2 → [BaO]−$(NO_2)(NO_3)$	−55	−50
[BaO] + $3NO_2$ → [BaO]−$(NO_2)(NO_3)$ + NO	−88	−93

intriguing point of comparison.[11] Fitting the observed NO_x uptake as a function of temperature and time to a postulated uptake mechanism, Fridell et al. derive microkinetic parameters for the NO_x adsorption process that closely match the observed uptake. While not detailed in terms of adsorption sites and structures, the mechanism includes features consistent with the models proposed here, including discrete chemisorbed NO_2 and NO_3 states as well as NO_2/NO_3 pairs. The energetics of the steps that produce NO_2 and NO_3 adsorbates can be inferred from the fitted forward and reverse activation energies and compared with those calculated here for the analogous reactions, as shown in Table 5. The experimental system and the BaO models differ in many important details, but despite these complications the observed and calculated reaction energies agree remarkably well. In particular, the Fridell et al. results imply a cooperative enhancement of NO_2 adsorption by NO_3 of 17 kcal mol^{-1} (the difference between the first and third reaction energies in Table 5) which compares very favorably with the 15 kcal mol^{-1} calculated here. The comparison supports the qualitative and even quantitative validity of the model results.

From an application perspective, a key objective is the calculation of descriptors that correlate with the properties of interest—in this case, the affinity of an oxide for NO_x, in particular relative to SO_x and CO_2. Figure 10 plots the known standard formation enthalpies[38]of the bulk carbonates, nitrates, and sulfates from the oxides against the calculated formation energies of the surface adsorbates with the same stoichiometry. The expected trends in stability are readily evident, including the increase in stability from carbonate to nitrate to sulfate and from MgO to CaO to SrO to BaO. More remarkable is the linear relation between surface and bulk reaction energies. Excluding the calculated physisorption of CO_2 on MgO, the bulk exceed the surface energies by 11% with a correlation coefficient greater than 0.99. The exact scaling has contributions from the GGA and other model assumptions and is only directional. The linear correlation, however, implies that the surface and bulk reaction energies are determined by the same effects, i.e., by the local Lewis acid−base and electron-transfer interactions discussed above, and that nonlocal, electrostatic (Madelung) differences enter at most as a multiplicative constant. The largest outlier to the correlation is $Ba(NO_3)_2$; the energy plotted is for the NO_2/ionic NO_3 configuration shown in Figure 7d, and the "ionic" component may not be representative of the bulk chemistry. Substituting the NO_2/basic NO_3 energy shifts the $Ba(NO_3)_2$ point onto the line and improves the correlation even further. In contrast, ignoring the cooperative surface interaction by treating the NO_2 and NO_3 surface species in isolation depresses the nitrate surface energies by 20 kcal mol^{-1}, far off the line.

These results lend support to the use of (001) surface models for exploring trends in NO_x storage on oxides. They also highlight the practical challenges in designing a sulfur-resistant NO_x adsorbant material. Sulfates are more stable on alkaline earth oxide surfaces and in the bulk than nitrates, and the preference for sulfates scales with adsorption energies (Figure 10): the sulfate−nitrate difference is smallest at MgO, but the nitrate affinity is also the smallest here, implying desorption temperatures potentially too low for practical use. The linear relation between surface and bulk energies suggests that mixed oxides of the alkaline earths will at best move NO_x and SO_x adsorption along the same line, and that tuning of sulfate−nitrate stability will require moving beyond the alkaline earth oxide family. The situation is far from hopeless, however. On the contrary, the electron transfer and cooperative effects that distinguish the NO_x chemistry from that of CO_2 and SO_x are handles to be exploited in designing adsorbents with preferential NO_x affinity.

Conclusions

Computational results and comparison with experiment presented here provide new insight into the factors that control CO_2, SO_x, and NO_x adsorption on the alkaline earth oxides MgO through BaO. Simple Lewis acid−base concepts suffice to explain trends in surface and bulk reaction of the oxides with CO_2 and SO_x. Odd electron NO_x adsorbates require one-electron oxidation or reduction to enhance their acidity or basicity, and NO_x adsorption behavior is thus controlled in part by the ability to reduce or oxidize the adsorbing surface or nearby adsorbates. As a result, a variety of NO_x adsorption geometries are possible and pronounced cooperative interactions exist, whereby electron transfer between two NO_x adsorbates in close proximity actually enhances the adsorption energy of the pair over two adsorbates in isolation. This cooperative effect is most pronounced for the least basic member of the alkaline earth oxide series, MgO, but has a significant contribution even for BaO.

The notion of a cooperative enhancement driven by charge transfer has a number of precedents. Similar "proximity" effects have been predicted in the coadsorption of metal cations and inorganic anions on metal sulfides,[39,40] and electropositive and electronegative adatoms have long been known to influence molecular adsorption at metal surfaces through strong electrostatic interactions.[41] The possibly unique feature of NO_x adsorbates is their ability to act both as electron donor and acceptor—a consequence of low ionization energies and high electron affinities—and thus their ability to "self-enhance."

The qualitative and quantitative insights provided by this work provide a framework for understanding the factors that control adsorption phenomena of interest for selective NO_x trapping for environmental emissions control. Most importantly, they demonstrate fundamental differences in the properties that control NO_x adsorption compared to SO_x and CO_2—differences that may be exploitable in materials with more desirable NO_x adsorption properties. Further work is necessary to explore the extension of these concepts to materials outside the alkaline earth oxide family, and these extensions are the subject of ongoing investigation.

Acknowledgment. Many thanks are extended to Lars Pettersson and Elly Karlsen (University of Stockholm) and José Rodriguez (Brookhaven National Laboratory) for sharing results prior to publication, and to Chris Goralski, Pete Schmitz, John Li, Dairene Uy, and Ken Hass (Ford Motor Company), John Gland (University of Michigan), and Marina Miletic (University of Illinois) for many helpful conversations regarding NO_x adsorption on oxides.

References and Notes

(1) Brown, G. E., Jr.; Henrich, V. E.; Casey, W. H.; Clark, D. L.; Eggleston, C.; Felmy, A.; Goodman, D. W.; McCarthy, M. I.; Maciel, G.; McCarthy, M. I.; Nealson, K. H.; Sverjensky, D. A.; Toney, M. F.; Zachara, J. M. *Chem. Rev.* **1999**, *99*, 77.

(2) Henrich, V. E.; Cox, P. A. *The Surface Science of Metal Oxides*; Cambridge University Press: Cambridge, 1994.

(3) Miyoshi, N.; Matsumoto, S.; Katoh, K.; Tanaka, T.; Harada, J.; Takahashi, N.; Yokota, K.; Sugiura, M.; Kasahara, K. *Soc. Automot. Eng.* **1995**, 19950809.

(4) Pacchioni, G.; Ricart, J. M.; Illas, F. *J. Am. Chem. Soc.* **1994**, *116*, 10152.

(5) Schneider, W. F.; Li, J.; Hass, K. C. *J. Phys. Chem. B* **2001**, *105*, 6972.

(6) Rodriguez, J. A.; Jirsak, T.; Freitag, A.; Larese, J. Z.; Maiti, A. *J. Phys. Chem. B* **2000**, *104*, 7439.

(7) Pacchioni, G.; Clotet, A.; Ricart, J. M. *Surf. Sci.* **1994**, *315*, 337.

(8) Karlsen, E. J.; Nygren, M. A.; Pettersson, L. G. M. *J. Phys. Chem. B* **2003**, *107*, 7795.

(9) Schneider, W. F.; Hass, K. C.; Miletic, M.; Gland, J. L. *J. Phys. Chem. B* **2002**, *106*, 7405.

(10) Miletic, M.; Gland, J. L.; Schneider, W. F.; Hass, K. C. *J. Phys. Chem. B* **2003**, *107*, 157.

(11) Olsson, L.; Persson, H.; Fridell, E.; Skoglundh, M.; Andersson, B. *J. Phys. Chem. B* **2001**, *105*, 6895.

(12) Kresse, G.; Furthmüller, J. *Comput. Mater. Sci.* **1996**, *6*, 15.

(13) Kresse, G.; Joubert, J. *Phys. Rev. B* **1999**, *59*, 1758.

(14) Blöchl, P. E. *Phys. Rev. B* **1994**, *50*, 17953.

(15) Perdew, J. P.; Wang, Y. *Phys. Rev. B* **1992**, *45*, 13244.

(16) Perdew, J. P.; Chevary, J. A.; Vosko, S. H.; Jackson, K. A.; Pederson, M. R.; Singh, D. J.; Fiolhais, C. *Phys. Rev. B* **1992**, *46*, 6671.

(17) Wyckoff, R. W. G. *Crystal Structures*; Wiley: New York, 1963.

(18) Baranov, A. N.; Stepanyuk, V. S.; Hergert, W.; Katsnelson, A. A.; Settels, A.; Zeller, R.; Dederichs, P. H. *Phys. Rev. B* **2002**, *66*, 155117.

(19) Pacchioni, G. *Surf. Sci.* **1993**, *281*, 207.

(20) Wells, A. F. *Structural Inorganic Chemistry*, 5th ed.; Clarendon Press: Oxford, 1984.

(21) Wichtendahl, R.; Rodriguez-Rodrigo, M.; Härtel, U.; Kuhlenbeck, H.; Freund, H.-J. *Phys. Status Sol.* **1999**, *173*, 93.

(22) Rodriguez, J. A.; Jirsak, T.; Pérez, M.; González, L.; Maiti, A. *J. Chem. Phys.* **2001**, *114*, 4186.

(23) Di Valentin, C.; Pacchioni, G.; Chiesa, M.; Giamello, E.; Abbet, S.; Heiz, U. *J. Phys. Chem. B* **2002**, *106*, 1637.

(24) Lu, X.; Xu, X.; Wang, N.; Zhang, Q. *J. Phys. Chem. B* **1999**, *103*, 5657.

(25) Snis, A.; Panas, I. *Surf. Sci.* **1998**, *412/413*, 477.

(26) Greenwood, N. N.; Earnshaw, A. *Chemistry of the Elements*, 2nd ed.; Butterworth-Heinemann: Oxford, 1997.

(27) Rodriguez, J. A.; Jirsak, T.; Kim, J.-Y.; Larese, J. Z.; Maiti, A. *Chem. Phys. Lett.* **2000**, *330*, 475.

(28) Rodriguez, J. A.; Jirsak, T.; Sambasivan, S.; Fischer, D.; Maiti, A. *J. Chem. Phys.* **2000**, *112*, 9929.

(29) Broqvist, P.; Panas, I.; Fridell, E.; Persson, H. *J. Phys. Chem. B* **2002**, *106*, 137.

(30) Bartmess J. E. *NIST Chemistry Webbook, NIST Standard Reference Database Number 69*; National Institutes of Standards and Technology: Gaithersburg, MD, 2001.

(31) Karlsen, E. J.; Nygren, M. A.; Pettersson, L. G. M. *J. Phys. Chem. A* **2002**, *106*, 7868.

(32) Di Valentin, C.; Pacchioni, G.; Abbet, S.; Heiz, U. *J. Phys. Chem. B* **2002**, *106*, 7666.

(33) Rodriguez, J. A. *Theor. Chem. Acc.* **2002**, *107*, 117.

(34) Schmitz, P. J.; Baird, R. *J. Phys. Chem. B* **2002**, *106*, 4172.

(35) Hess, C.; Lunsford, J. H. *J. Phys. Chem. B* **2002**, *106*, 6358.

(36) Low, M. D. J.; Yang, R. T. *J. Catal.* **1974**, *34*, 479.

(37) Underwood, G. M.; Miller, T. M.; Grassian, V. H. *J. Phys. Chem. A* **1999**, *103*, 6184.

(38) *CRC Handbook of Chemistry and Physics*, 84th ed.; CRC Press: Boca Raton, 2003.

(39) Becker, U.; Rosso, K. M.; Hochella, J. M. F. *Geochim. Cosmochim. Acta* **2001**, *65*, 2641.

(40) Rosso, K. M.; Becker, U. *Geochim. Cosmochim. Acta* **2003**, *67*, 941.

(41) Lang, N. D.; Holloway, S.; Nørskov, J. K. *Surf. Sci.* **1985**, *150*, 24.